Supporting Information:

Low-Frequency (1/*f*) Noise in Nanocrystal Field-Effect Transistors

Yuming Lai,[1] Haipeng Li,[1] David K. Kim,[2] Benjamin T. Diroll,[3] Christopher B. Murray,[2,3], Cherie R. Kagan[1,2,3,]*

[1]Department of Electrical and Systems Engineering, University of Pennsylvania, Philadelphia, PA; [2]Department of Materials Science and Engineering, University of Pennsylvania, Philadelphia, PA; [3]Department of Chemistry, University of Pennsylvania, Philadelphia, PA

**To whom correspondence should be addressed. E-mail: kagan@seas.upenn.edu*

Discussion

Calculation of Carrier Mobility for Saturation and Linear regimes[1]

In the linear regime (V_{GS}-V_T > V_{DS} > 0), carrier mobility is determined by

$$\mu_{LIN} = \frac{1}{C_{ox}\frac{L}{W}V_{DS}}\left(\frac{\partial I_D}{\partial V_{GS}}\right)$$

where C_{ox} is oxide capacitance, L is channel length, and W is channel width. In the saturation regime (V_{DS} > V_{GS}-V_T > 0), carrier mobility is determined by

$$\mu_{SAT} = \frac{2}{C_{ox}\frac{L}{W}}\left(\frac{\partial I_D^{1/2}}{\partial V_{GS}}\right)^2$$

Length Dependence of S_I/I_D^2

For a homogenous semiconductor, the noise expression[2,3] can be presented as

$$\frac{S_I}{I_D^2} = \frac{S_R}{R^2} = \frac{S_{Rchannel}+S_{Rcontact}}{(R_{channel}+R_{contact})^2} = \frac{\alpha}{Nf} \quad (1)$$

where $S_{Rchannel}$ and $S_{Rcontact}$ represent two uncorrelated noise sources and $R_{channel}$ and $R_{contact}$ are the channel and contact resistances. Using $\frac{S_R}{R^2} = \frac{\alpha}{Nf}$ relationship, $S_{Rchannel} = \frac{\alpha_{channel}R_{channel}^2}{N_{channel}f}$ and $S_{Rcontact} = \frac{\alpha_{contact}R_{contact}^2}{N_{contact}f}$ can be derived, where N is defined as free carriers in the channel or contact region. The carrier concentrations and resistances in the channel or contact regions are related to the transistor channel length (L) and width (W), and can be simplified as $N_{ch} \propto L \times W$, $N_{contact} \propto \frac{1}{W}$, $R_{ch} \propto \frac{L}{W}$ and $R_{contact} \propto \frac{1}{W}$.[2,3] Depending on the magnitude of each term, Equation 1 can be simplified into four possible expressions.

$R_{channel} > R_{contact}$, $S_{Rchannel} > S_{Rcontact}$ $\quad \frac{S_I}{I_D^2} = \frac{S_R}{R^2} = \frac{S_{Rchannel}}{R_{channel}^2} \propto \frac{1}{L \times W}$

$R_{channel} > R_{contact}$, $S_{Rcontact} > S_{Rchannel}$ $\quad \frac{S_I}{I_D^2} = \frac{S_R}{R^2} = \frac{S_{Rcontact}}{R_{channel}^2} \propto \frac{W}{L^2}$

$R_{contact} > R_{channel}$, $S_{Rchannel} > S_{Rcontact}$ $\quad \frac{S_I}{I_D^2} = \frac{S_R}{R^2} = \frac{S_{Rchannel}}{R_{contact}^2} \propto \frac{L}{W}$

$R_{contact} > R_{channel}$, $S_{Rcontact} > S_{Rchannel}$ $\quad \frac{S_I}{I_D^2} = \frac{S_R}{R^2} = \frac{S_{Rcontact}}{R_{contact}^2} \propto W$

With the assumption of a constant value of W or W/L, Table 2 in the main text is derived.

Stretched Exponential Function

Bias-stress effects are typically described by a stretched exponential function[4,5] as

$$\Delta V_T = (V_{GS} - V_{T0})\{1 - exp[-(t/\tau)^{\beta}]\} \quad (2)$$

where ΔV_T is threshold voltage (V_T) shift under constant gate-source (V_{GS}) and drain-source bias (V_{DS}) for an extended period of time. V_{T0} is the initial value of V_T, t is the time the stress is applied, and τ and β are fitting parameters. This equation can be converted to express bias-stress induced current degradation *via* current expressions for ideal thin-film transistors[1]. For example, the initial saturation current is

$$I = \frac{1}{2}\mu C_{ox}\frac{W}{L}(V_{GS} - V_{T0})^2 = k(V_{GS} - V_{T0})^2 \quad (3)$$

and changes to

$$I' = \frac{1}{2}\mu C_{ox}\frac{W}{L}[V_{GS} - (V_{T0} + \Delta V_T)]^2 = k[V_{GS} - (V_{T0} + \Delta V_T)]^2 \quad (4).$$

Expanding Equation (4) and using Equation (2) and (3), the saturation current degradation as a function of time is $\frac{I'}{I} = \exp\left[-2(t/\tau)^{\beta}\right]$. Using the initial linear current

$$I = \frac{1}{2}\mu C_{ox}\frac{W}{L}[2(V_{GS} - V_{T0})V_{DS} - V_{DS}^2] \quad (5)$$

a similar function for linear current degradation can be derived as $\frac{I'}{I} = \exp\left[-\left(t/\tau\right)^{\beta}\right]$, assuming $(V_{DS})^2$ is negligible. These two equations are applied to fit the time dependence of the drain-source current (I_D) in Figure S5. It is obvious that encapsulated devices have orders of magnitude higher value of τ than unencapsulated devices, suggesting encapsulated devices are more stable under bias-stress.

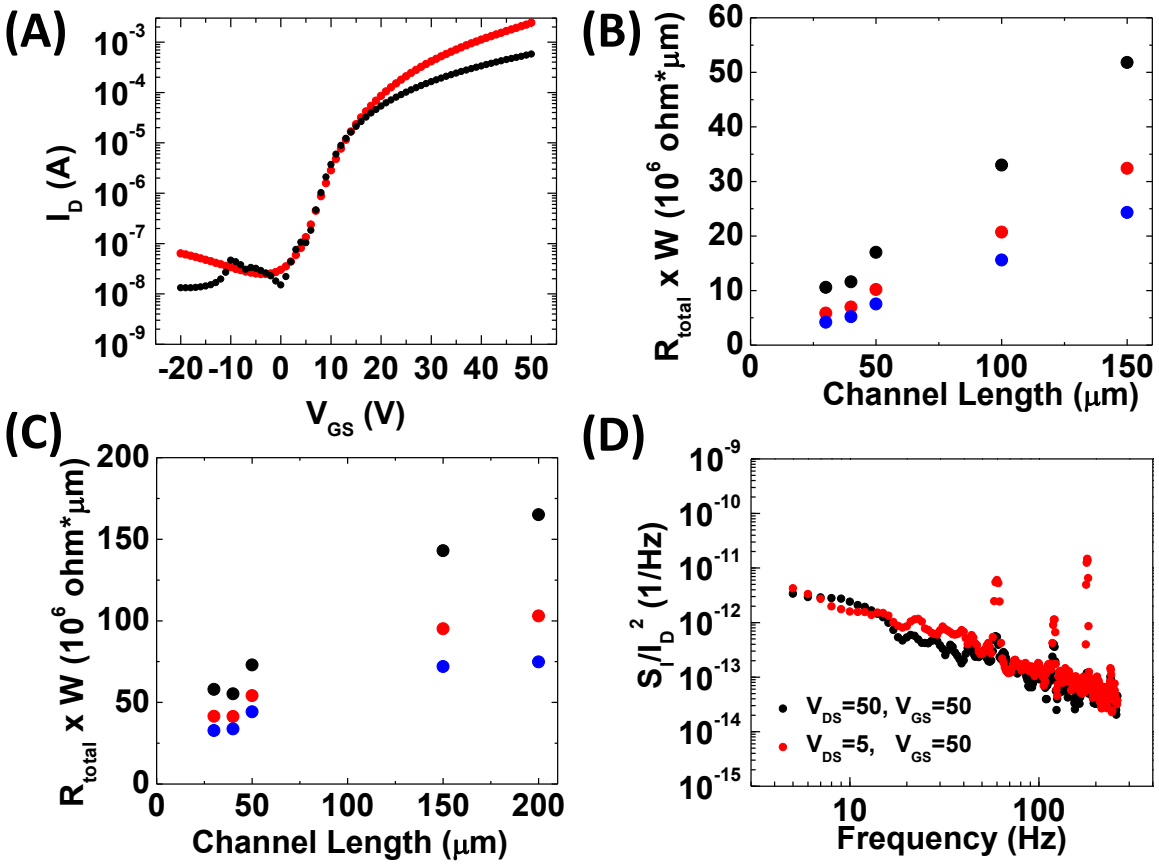

Figure S1. (A) Representative transfer characteristics (I_D-V_{GS}) for top-contact (red) and bottom-contact (black) devices, with L = 50 μm and measured at V_{DS} = 50 V. The contact ($R_{contact}$) and channel ($R_{channel}$) resistances are extracted from the total resistance (R_{total}) as a function of channel length using the transmission line method for (B) top-contact and (C) bottom-contact devices respectively, collected at V_{GS} = 30 V (black), V_{GS} = 40 V (red), and V_{GS} = 50 V (blue). (D) A representative S_I/I_D^2 *vs* frequency of a top-contact, L = 40 μm device measured in the saturation and linear regimes, showing that noise is weakly dependent on V_{DS}.

Channel Length (μm)	V_{GS} = 40 V			V_{GS} = 30 V		
	R_{total} (Ω)	$\frac{R_{contact}}{W}$ (Ω)	Mobility (cm^2/Vs)	R_{total} (Ω)	$\frac{R_{contact}}{W}$ (Ω)	Mobility (cm^2/Vs)
30	$1.2x10^4$	$-2.2x10^3$	19.73	$2.1x10^4$	$-3.9x10^2$	11.57
40	$1.2x10^4$	$-1.6x10^3$	19.45	$2.1x10^4$	$-2.9x10^2$	12.01
50	$1.3x10^4$	$-1.3x10^3$	17.29	$2.1x10^4$	$-2.3x10^2$	12.67
100	$1.3x10^4$	$-6.6x10^2$	15.75	$2.2x10^4$	$-1.1x10^2$	15.01
150	$1.4x10^4$	$-4.4x10^2$	15.01	$2.2x10^4$	-78.2	14.77

Table S1. Device resistances extracted by the transmission line method and carrier mobilities for top-contact devices at V_{GS} = 40 V and V_{GS} = 30 V.

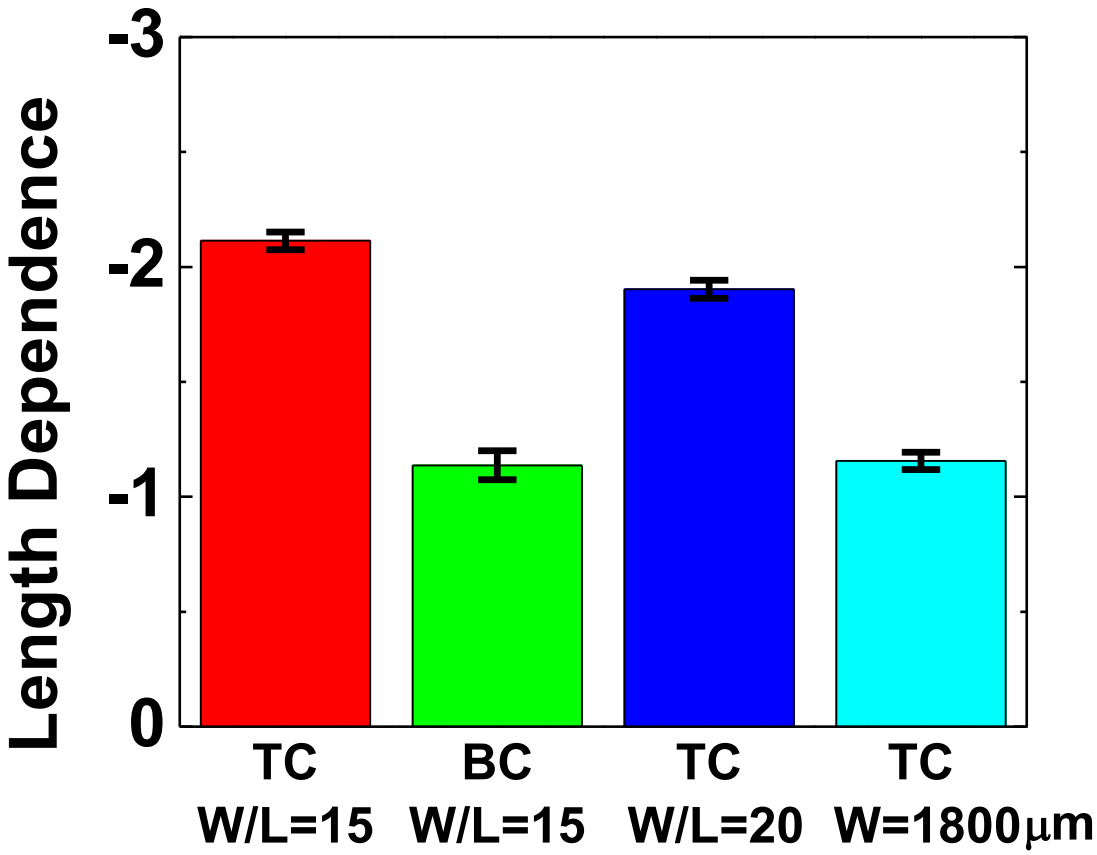

Figure S2. Statistics of the length dependence of S_I/I_D^2 for different scaling of the device geometry.

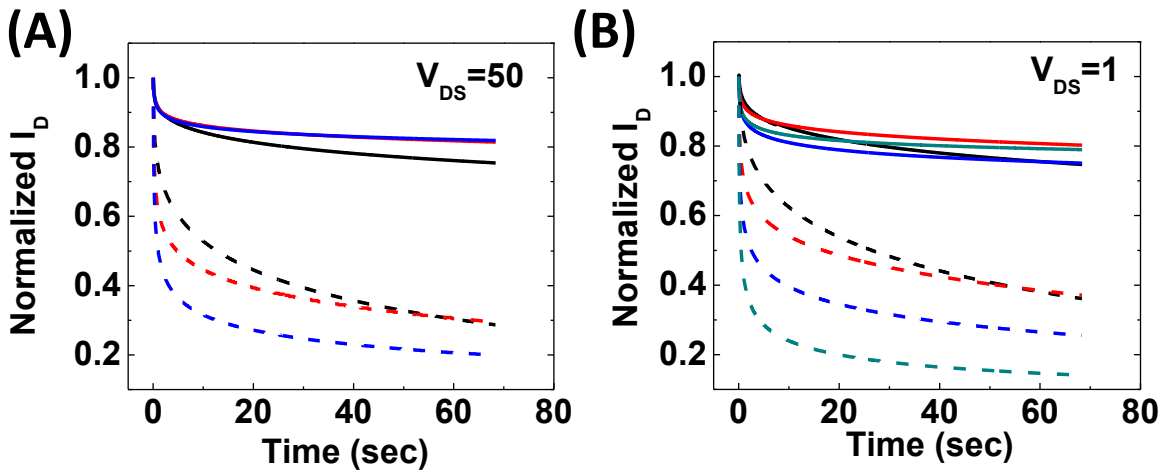

Figure S3. Time dependence of the normalized drain-source current (I_D) measured under a voltage stress of (A) V_{DS} = 50 V and (B) V_{DS} = 1 V for an unencapsulated, top-contact device (dashed lines) and an Al_2O_3-encapsulated, top-contact device (solid lines), where V_{GS} = 50 V (black), V_{GS} = 40 V (red), V_{GS} = 30 V (blue) and V_{GS} = 20 V (green).

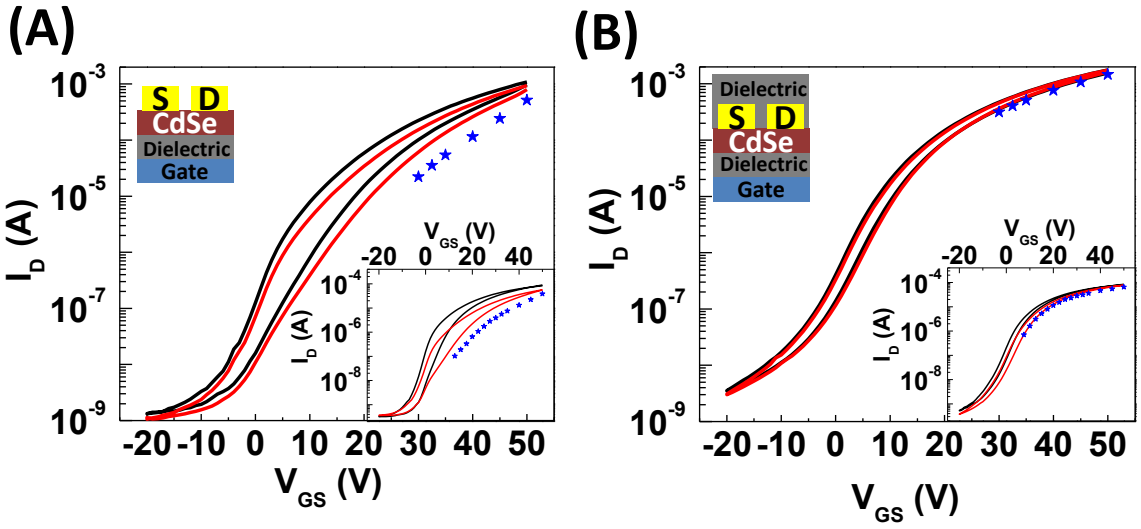

Figure S4. Device transfer characteristics I_D-V_{GS} for (A) an unencapsulated, top-contact and (B) an Al_2O_3-encapsulated, top-contact device at V_{DS} = 50 V and V_{DS} = 1 V (inset), where I_D-V_{GS} before (black) and after (red) noise collection are presented. The average stress current during noise collection is shown as blue stars at each applied bias and is the average of the current collected in Fig. S3 from 10 sec to the end of applied bias at 70 sec. Note: the calculated interface trap density from the subthreshold swing is 9.67 x 10^{12} cm^{-2} for (A) and 9.14 x 10^{12} cm^{-2} for (B).

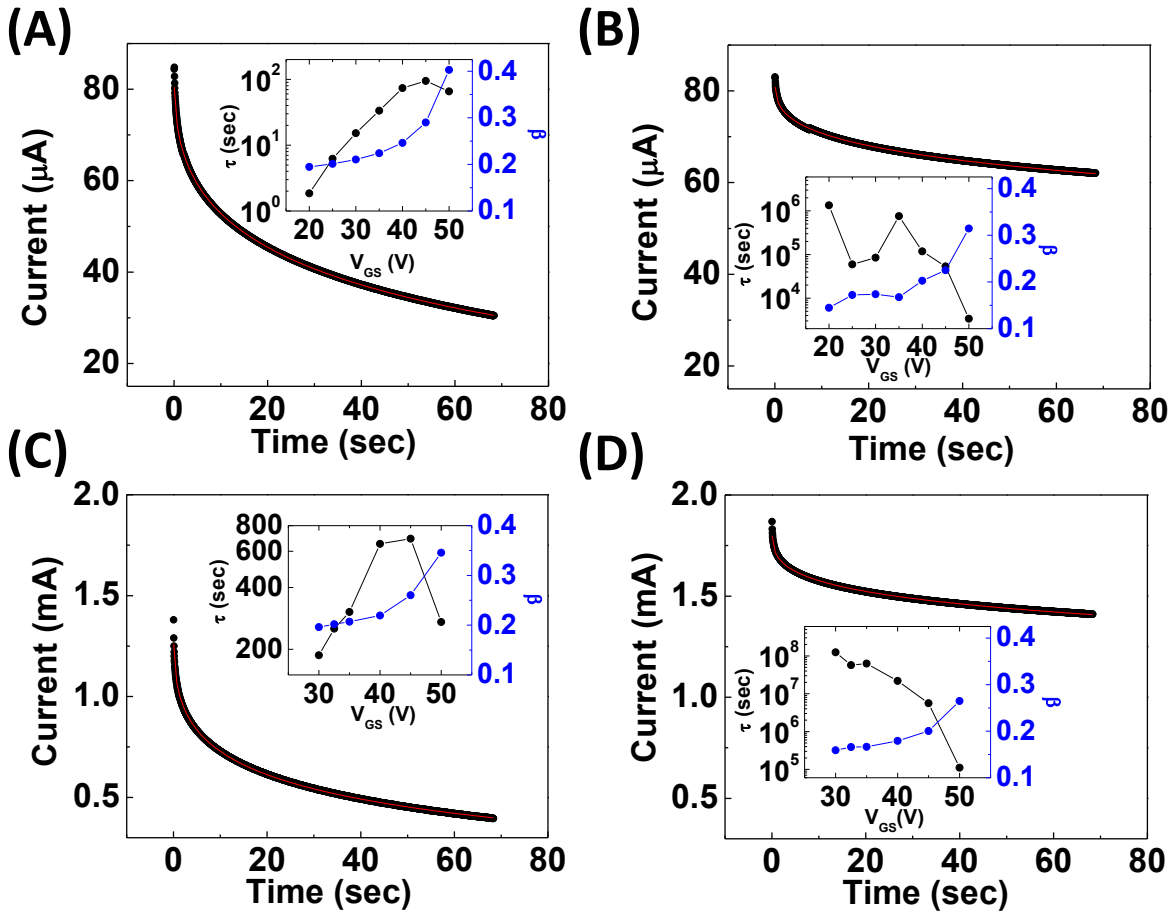

Figure S5. Traces of I_D as a function of time under voltage stress (black) and fits to a stretched exponential function (red) for (A) an unencapsulated, top-contact and (B) an Al_2O_3-encapsulated, top-contact device under V_{DS} = 1 V, V_{GS} = 50 V and for (C) an unencapsulated, top-contact device and (D) an Al_2O_3-encapsulated, top-contact device under V_{DS} = 50 V, V_{GS} = 50 V. Insets in (A-D) show fitting parameters (τ and β) as a function of V_{GS}.

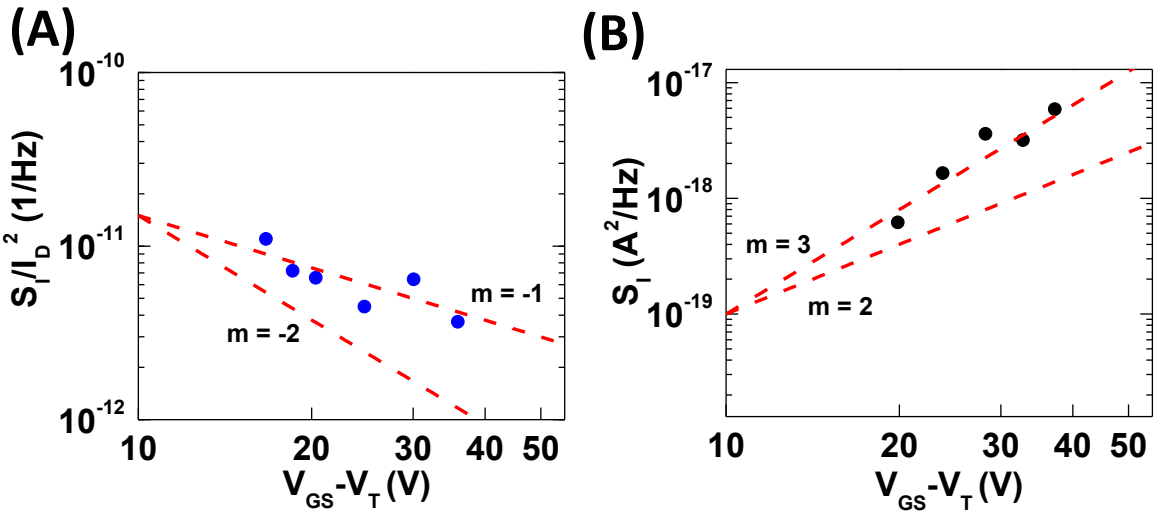

(C)

	Linear Regime	Saturation Regime
Δμ	$\frac{S_I}{I_D^2} \propto \frac{t_i}{WL(V_{GS}-V_T)}$	$S_I \propto \frac{(V_{GS}-V_T)^3}{t_i^3}\frac{W}{L^3}$
ΔN	$\frac{S_I}{I_D^2} \propto \frac{t_i^2}{WL(V_{GS}-V_T)^2}$	$S_I \propto \frac{(V_{GS}-V_T)^2 W}{L^3}$

Figure S6. (A) Representative S_I/I_D^2 *vs* (V_{GS}-V_T) characteristics at a frequency of 10 Hz for an Al_2O_3-encapsulated device operated in the linear regime (V_{DS} = 1 V). The slope fit for frequencies between 5 to 10 Hz in a step of 1 Hz is -0.9 ± 0.15. Slopes of -1 and -2 are drawn for reference. (B) Representative S_I *vs* (V_{GS}-V_T) at a frequency of 10 Hz for an Al_2O_3-encapsulated device operated in the saturation regime (V_{DS} = 50 V). The slope fit for frequencies between 5 to 10 Hz in a step of 1 Hz is 3.1 ± 0.27. Slopes of 2 and 3 are drawn for reference. (C) Comparison of the S_I/I_D^2 and S_I dependence on (V_{GS} -V_T) for the Hooge (Δμ) and McWhorter (ΔN) models for devices operated in linear and saturation modes.[6]

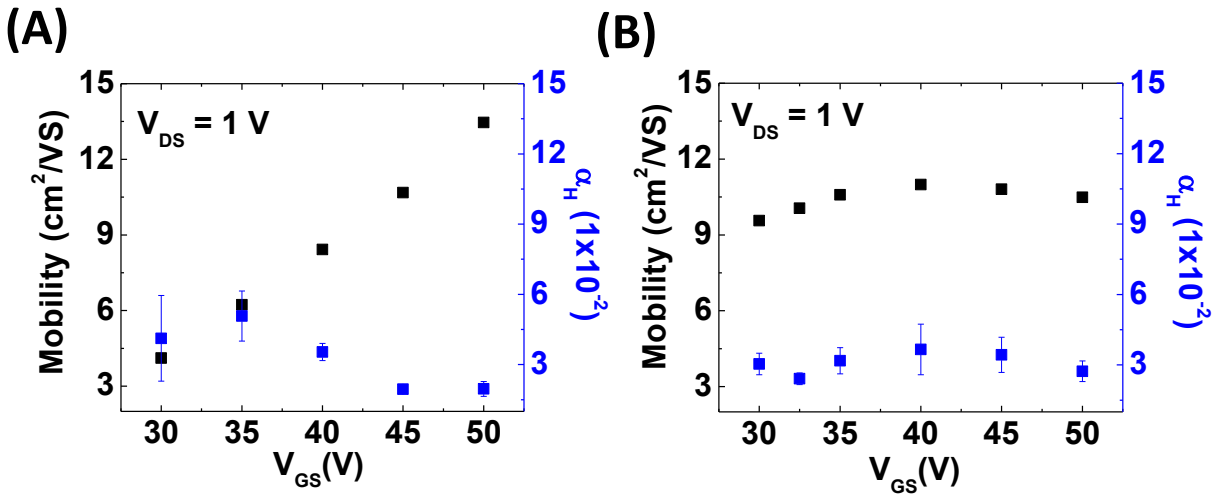

Figure S7. Mobility and Hooge parameter (α_H) as a function of V_{GS} when V_{DS} = 1 V for (A) unencapsulated, top-contact and (B) Al_2O_3-encapsulated, top-contact devices.

Reference

(1) Sze, S. M.; Kwok, K. *Physics of Semiconductor Devices, 3rd Edn*; Edition, 3rd, Ed.; John Wiley & Sons, 2007.

(2) Peransin, J.; Vignaud, P.; Rigaud, D.; Vandamme, L. K. J. L/f Noise in MODFET's at Low Drain Bias. *IEEE Trans. Electron Devices* **1990**, *37*, 2250–2253.

(3) Rhayem, J.; Valenza, M.; Rigaud, D.; Szydlo, N.; Lebrun, H. 1/f Noise Investigations in Small Channel Length Amorphous Silicon Thin Film Transistors. *J. Appl. Phys.* **1998**, *83*, 3660.

(4) Shih, C.-C.; Lee, Y.-S.; Fang, K.-L.; Chen, C.-H.; Gan, F.-Y. A Current Estimation Method for Bias-Temperature Stress of a-Si TFT Device. *IEEE Trans. Device Mater. Reliab.* **2007**, *7*, 347–350.

(5) Zschieschang, U.; Weitz, R. T.; Kern, K.; Klauk, H. Bias Stress Effect in Low-Voltage Organic Thin-Film Transistors. *Appl. Phys. A* **2008**, *95*, 139–145.

(6) Rigaud, D.; Valenza, M.; Rhayem, J. Low Frequency Noise in Thin Film Transistors. *IEE Proc. - Circuits, Devices Syst.* **2002**, *149*, 75–82.